A HIGH-REYNOLDS-NUMBER SEAL TEST FACILITY: FACILITY DESCRIPTION AND PRELIMINARY TEST DATA*

Dara W. Childs, Clayton Nelson, and Ted Noyes
Department of Mechanical Engineering
Texas A&M University
College Station, Texas 77843

John B. Dressman
Department of Mechanical Engineering
The University of Louisville
Louisville, Kentucky 40229

ABSTRACT

A facility has been developed for testing the leakage and rotordynamic characteristics of interstage-seal configurations for the HPFTP (High Pressure Fuel Turbopump) of the SSME (Space Shuttle Main Engine). Axial Reynolds numbers on the order of 400,000 are realized in the test facility by using a Dupont freon fluid called Halon ($CBrF_3$). The kinematic viscosity of Halon is of the same order as the liquid hydrogen used in the HPFTP. Initial testing has focused on the current flight configurations (a three-segment, stepped unit) and a convergent-taper candidate.

INTRODUCTION

The HPFTP development program experienced considerable difficulty with subsynchronous, unstable vibration problems [1]. As originally designed, the HPFTP was violently and destructively unstable at running speeds above approximately 20,000 rpm. The remedy for this situation consisted of the following steps: (a) the original soft bearing carriers were replaced by stiff bearing carriers, and (b) the grooving was removed from the original stepped interstage seal design. With these modifications, the HPFTP has been stable over its design speed range. The essential contribution of the seal modification to the elimination of the rotor instability was underlined by tests in 1979 on an HPFTP unit which whirled enthusiastically after the interstage seal clearances were deliberately enlarged.

From a rotordynamics viewpoint, seal analysis has the objective of predicting the influence-coefficients of the following equations:

$$-\begin{Bmatrix} R_X \\ R_Y \end{Bmatrix} = \begin{bmatrix} K & k \\ -k & K \end{bmatrix} \begin{Bmatrix} r_X \\ r_Y \end{Bmatrix} + \begin{bmatrix} C & c \\ -c & C \end{bmatrix} \begin{Bmatrix} \dot{r}_X \\ \dot{r}_Y \end{Bmatrix} + \begin{bmatrix} M & m \\ -m & M \end{bmatrix} \begin{Bmatrix} \ddot{r}_X \\ \ddot{r}_Y \end{Bmatrix} \qquad (1)$$

*The work reported herein was supported by NASA Contract NAS8-33176 from George C. Marshall Space Flight Center, Alabama 35812; Contract Monitor: Frank Garcia.

as a function of seal operating conditions. Initial analyses and testing for interstage and wearing seals were published by Black et al. [2-5]. Black used the following leakage relationship from Yamada [6]:

$$\Delta P = \frac{\rho V^2}{2} [1+\xi+2\sigma] \tag{2}$$

where ξ is a constant entry-loss coefficient, V is the average fluid velocity, and σ is the friction-loss coefficient defined by;

$$\sigma = \frac{\lambda L}{C_r} \quad . \tag{3}$$

In this relationship, L is the seal length, C_r is the radial clearance, and λ is the following function of the axial and circumferential Reynolds numbers (R_a,R_c):

$$\lambda = 0.079\ R_a^{-1/4}[1+(\frac{7R_c}{8R_a})^2]^{3/8}$$

$$R_a = 2VC_r/\nu,\ R_c = R\omega C_r/\nu \tag{4}$$

where ν is the fluid's kinematic viscosity, R is the seal radius, and ω is the rotor's rotational speed.

Childs has subsequently developed analyses [7,8] for constant clearance seals based on Hirs' turbulent lubrication equations [9]. These results are similar to Black's, but differ in some respects. Their principal advantage is in a direct derivation from a single set of governing equations.

Fleming [10] proposed that the direct stiffness of seals could be increased by either (a) introducing a step in a constant-clearance seal, or (b) using a convergent-taper geometry. Childs [11] completed an analysis for convergent-tapered seals which defined all of the dynamic coefficients, and demonstrated that the seal taper significantly reduces the seal damping and cross-coupled stiffness terms, while increasing the direct stiffness. Hendricks [12] found in testing straight and convergent tapered seals at large eccentricities in liquid hydrogen that a slight taper reduced local seal cavitation at the seal exit, and eliminated the possibility of a local negative stiffness developing.

Black's analysis was used initially in predicting the rotordynamic coefficients of the HPFTP interstage seals [1]. His experimental results were for plain (constant-clearance) seals having smooth and serrated surfaces, and extended out to axial Reynolds numbers on the order of 20,000, as compared to 500,000 for the HPFTP. Given that the HPFTP seals differ substantially from those tested by Black in both configuration and operating conditions, the decision was made to implement a test program to directly measure the forces developed by seals, which are geometrically similar to the HPFTP seals and operating at the same Reynolds number conditions. The development of a facility to make these measurements together with a discussion of some preliminary results is the subject of this report.

FACILITY DESCRIPTION

Test Section

The test section design is an extension of an earlier design used in a University of Louisville test program [13], and is illustrated in Figure 1. Fluid enters in the center and discharges axially across the two test seals. The seals on the right and left illustrate, respectively, the current stepped configuration and a proposed convergent-tapered configuration for the HPFTP interstage seals. The current test section differs from that employed earlier [13] in that it assembles in a mid-plane position, which permits testing of the "slingers" shown in the figure.

The test-section rotor is supported in Torrington hollow-roller bearings* [14], which are extremely precise, radially preloaded, and have a predictable and repeatable radial stiffness. The test seals are mounted eccentrically to the test rotor; hence, rotor rotation develops a rotating pressure field that is constant with respect to a rotor-fixed observer. Axially-spaced kulite strain-gauge pressure transducers are used to measure the pressure field which is developed by seal rotation. Seal motion is measured by MTI capacitance probes in the vertical and horizontal planes. Inlet and discharge measurements are made of temperature and pressure for use in defining the density and viscosity of the test fluid.

A 10-hp variable-speed electric motor is used to drive the test section from five rpm to 5300 rpm. A motion transducer, actuated by a rotating ten-toothed wheel, provides a signal for a counter which defines the rpm of the test section.

John Dressman of the University of Louisville designed the test section and supervised its construction.

Test-Fluid Selection

The very high Reynolds numbers encountered in the HPFTP result from (a) the extremely low kinematic viscosity of liquid hydrogen, (b) the high-shaft rotational speed, and (c) the very large ΔP's developed by the HPFTP stages. The average properties of hydrogen within the HPFTP interstage seals are

$$\mu = 1.16 \times 10^{-5} \text{ Ns/m}^2, \quad \rho = 71.2 \text{ kg/m}^2$$

$$\nu = 1.63 \times 10^{-7} \text{ m}^2/\text{sec}.$$

For comparison, the nominal properties of water at 25°C are

$$\mu = 8.9 \times 10^{-4} \text{ Ns/m}^2, \quad \rho = 1000 \text{ kg/m}^3$$

$$\nu = 8.9 \times 10^{-7} \text{ m}^2/\text{sec}.$$

Since the Reynolds numbers are inversely proportional to ν, an ideal test fluid should have a low absolute viscosity and a high density.

---

* These bearings were made available from Torrington, Incorporated through the courtesy of W. L. Bowen.

The test fluid selected to meet these criteria is bromotrifluoromethane, $CBrF_3$, which is manufactured as a fire extinguisher fluid (Dupont FE 1301 or Halon) and refrigerant (Freon 13B1). Its fluid properties at 25°C are [15,16]

$$\mu = 1.54 \times 10^{-4} \text{ Ns/m}^2, \quad \rho = 1570 \text{ kg/m}^3,$$

$$\nu = 1.0 \times 10^{-7} \text{ m}^2/\text{s}.$$

This liquid actually has a lower kinematic viscosity than liquid hydrogen, and has the additional advantage of being nonflammable and nontoxic. The vapor pressure of Halon is approximately 200 psi at room temperature.

Seal Geometry

As illustrated in Figure 1, the current flight geometry uses three constant-clearance seal segments separated by two steps. The dimensions of the test seal segments are

L_i (cm)	R_i (cm)	C_{ri} (mm)
1.4986	5.0292	0.5080
1.5265	4.9682	0.5080
1.8034	4.9098	0.4826

The dimensions of the tapered seal are

$$L = 4.996 \text{ cm}, \quad R = 5.0292,$$

$$C_{ro} = 0.5715 \text{ mm}, \quad C_{ri} = 0.4572 \text{ mm}$$

where C_{ro} and C_{ri} are the entrance and exit clearances, respectively. These dimensions yield the following definition for the tapered parameter:

$$q = (C_{ro}-C_{ri})/(C_{ro}+C_{ri}) = 0.111.$$

Relatively speaking, this is a slight taper which should [11] slightly increase K, while slightly decreasing the remaining coefficients.

Mechanical System Layout

Figure 2 illustrates the flow loop used to provide specified flowrates through the test-section seals. A six-stage Goulds pump provides the flowrate required. Loop flow rate discharges from the pump, and then may split with part of the flow going through the test section, and the remainder proceeding through control valves 1 and 3. Two control valves in series are required to absorb the full output pressure of the pump without cavitation. The bypass flow mode is used for total test-section flowrate less than 100 gpm, which represents the lowest flowrate operating point for the pump. Valve 4 is closed in the bypass mode. As the required flowrate increases above 100 gpm, valve 1 is closed and valves 2 and 3 are progressively opened. Valve 4, which has a larger capacity than the remaining valves, is opened to achieve maximum flow conditions. Flowrate through the test section seals is measured by Fischer-Porter vortex flowmeters.

The test-section fluid is circulated through a heat exchanger, which is supplied chilled water by a Trane chiller. The chiller capacity is augmented by a 2000 gallon water tank which is buried outside the test facility.

The ambient system pressure is maintained by the accumulators illustrated in Figure 2. They are also used to remove liquid Halon from the test section for replacement of rotors. Similar accumulators are used to transfer fluid back and forth from the 2000 lb Dupont delivery tank. In fact, all of the Halon can be pumped back into the delivery tank using the accumulators.

The filters illustrated in Figure 2 have a ten micron limit for particles. The complete flow system is stainless steel except for the pump body and the heat exchanger so that particle contamination in the test fluid is minimized.

Control System

The axial and circumferential Reynolds numbers are the quantities to be controlled in the seals. These variables are determined by the pressure and temperature measurements within the seal (which define ρ and μ), the seal rotational speed ω, and the flowrates through the seals. Control is supplied by means of a Data General Nova computer. Control signals are generated, based upon the difference between a measured R_a and a specified $\bar{R}_a$, and cause a change in the Masoniellan control values. Active control is not entirely closed-loop. The operator specifies the number of control cycles to be evaluated by the computer. The computer calculates the running speed that is required to achieve a specified $\bar{R}_c$, and the specified test section speed is set manually.

DATA ACQUISITION AND ANALYSIS

Data Acquisition System

The transient test data to be recorded consists of the seal motion $r_x(t)$, $r_y(t)$ and the pressure measurements $p_i(t)$. Five pressure measurements are made for the tapered seal, with their spacing specified by a Gauss-Legendre quadrature formula [13]. Four additional pressure measurements are made on the stepped seals to measure the pressure immediately upstream and downstream of the steps. These data are recorded using a 17-channel Physical Data, Inc. recorder. Each channel of this unit has its own A/D converter with a sampling rate up to 2×10^6 Hz, and 4096 storage locations.

The physical data system is controlled from the D. G. Nova computer, which enables the recorder, commands data capture, and then controls dumping of the data into disk memory of the Nova. Transient data for control of the system is obtained directly through A/D units on the Nova.

Data Analysis

As outlined in [13], transient data analysis consists of alignment of the pressure signals (which are measured at various circumferential locations), and integrating the pressure signals to obtain the seal force components. The test rig causes a synchronous precession of the seals, and the resultant motion may be stated:

$$r_X = A \cos \omega t, \quad r_Y = A \sin \omega t \tag{5}$$

The six coefficients of Eq. (1) can not be separately identified for this type of motion. In fact, if Eq. (5) is substituted into Eq. (1), and the coefficients of sin ωt and cos ωt on both sides of Eq. (1) are equated, only two independent numbers can be identified. For the present study, the two numbers chosen for presentation are the radial and circumferential components of the reaction force. From Equations (1) and (5) these components may be stated:

$$\begin{aligned} R_\theta/A &= \frac{|\bar{r} \times \bar{R}|}{A^2} = k - C\omega - m\omega^2 \\ R_r/A &= \frac{|\bar{r} \cdot \bar{R}|}{A^2} = M\omega^2 - c\omega - K \ . \end{aligned} \tag{6}$$

Since the coefficients depend on σ, which in turn depends on $R_c = R\omega C_r/\nu$, one can not generally vary ω to obtain additional independent equations for the solution of the coefficients. Stated differently, changing ω also changes the coefficients. An exception to this rule is provided by very high values of R_a for which σ is insensitive to changes in ω.

TEST SERIES

Three rotors were initially manufactured for use in testing the general seal configurations of Figure 1, viz , the current flight configuration and a tapered-seal alternative. These rotors differ only in the nominal seal eccentricity; specifically, they have the following eccentrities and eccentricity ratios:

(a) Rotor 1, A = .005 in, $A/C_r = 0.25$,

(b) Rotor 2, A = .010 in, $A/C_r = 0.50$, and

(c) Rotor 3, A = 0.0 in, $A/C_r = 0.0$.

The zero eccentricity rotor provides static leakage and pressure gradients only. Rotors 1 and 2 provide insight as to the influence of seal dynamic eccentricity on test results. The above rotors have been tested over the following nominal axial and circumferential Reynolds number ranges:

R_a: 50,000, 75,000, 150,000, 325,000, 400,000

R_c: 40,000, 65,000, 90,000, 115,000, 140,000

More specifically, a matrix of tests has been carried out such that all of the five values of R_c are obtained for each value of R_a.

Theoretical results [5,7,8] have demonstrated that the cross-coupling terms of Eq. (1), i.e., k, c, m, depend on the fluid tangential velocity entering the seal. The standard test rig provides minimal pre-rotation of the fluid entering the seal. Hence, rotor 2 was mofified by shrinking on an active "slinger" at the entrance to both seals to provide significant fluid pre-rotation. Slingers incorporated radial slots and an axial clearance of 0.010 in. for a radial distance

of 0.75 inches prior to seal entry. The power requirements to rotate this rotor are considerably higher than the other rotors, and data can only be taken for axial Reynolds numbers out to 150,000.

Two additional rotors have been manufactured to examine the influence of surface roughness on both sealing capability and the seal reaction-force components. These rotors have an "almost" circumferential grooving pattern with a nominal depth of 0.001 and 0.002 inches, respectively. The original, zero eccentric rotor, was machined to yield an 0.002 inch surface roughness pattern. All of these rotors have been tested over the complete Reynolds number range.

Additional planned tests include machining surface roughness into the housing, with the first and second machining operations yielding depths of 0.001 and 0.002 inches, respectively. The following rotors will be tested in these two surface-roughened housings:

(a) Rotor 1 (smooth); A = 0.005 in.,
(b) Rotor 4 (0.001 inches depth); A = 0.003 in.,
(c) Rotor 5 (0.002 inches depth); A = 0.005 in., and
(d) Rotor 3 (0.002 inches depth); A = 0.0 in.

Testing of helically grooved seals is proposed for the coming year which will include a systematic variation in taper angles, nominal clearances, and groove depths. Initial testing for these seals will be at zero eccentricities.

PRELIMINARY RESULTS

Reduction of the test data is still in a preliminary stage; hence, the results which are available for discussion are limited at present to some static data (ΔP - leakage and pressure gradients) and force magnitude results for the two seals of rotor 1.

Static Results

Static results were obtained for the stepped and tapered seals of rotor 3, viz., the zero-eccentricity rotor. Figures 3 and 4 illustrate the steady-state pressure gradients for the stepped and tapered seals, respectively, for a range of axial and circumferential Reynolds numbers. Each frame of these figure sets illustrates the influence of changes in R_c with R_a held constant. The strain-gauge pressure transducers used to obtain these results have an accuracy specifications of .1% of full scale, which amounts to approximately 1 psi. This lack of accuracy is much more noticeable at low flow rates and shallow pressure gradients than at high flow rates. To some extent, this explains the more "ragged" nature of the pressure gradients in the low flow conditions of figures 3 and 4 as compared to high flow conditions. Each data point in these figures corresponds to an average of 200 samples.

The pressure gradients of figures 3 and 4 are seen to be more sensitive to changes in R_c at low values of R_a, becoming relatively independent of R_c at higher values of R_a. This result would be expected, since from Eqs. (2) and (3)

$$\frac{\partial \sigma}{\partial R_c} = .045 \left(\frac{L}{C}\right) R_a^{-9/4} \left[1 + \left(\frac{7R_c}{8R_a}\right)^2\right]^{-5/8},$$

which shows a marked drop in sensitivity with increasing R_a.

An apriori analysis of the stepped seal for leakage would use Eq. (1) for each step yielding the results

$$\Delta P_i = \frac{\rho V_i^2}{2} (1 + \xi_i + 2\sigma_i); \; i = 1, 2, 3$$

$$\Delta P = \sum_{i=1}^{3} \Delta P_i$$

$$w = \rho V_i A_i \; ; \; i = 1, 2, 3$$

where A_i is the area of each annulus. Normally, one assumes that the entrance loss factors are constant, independent of R_a and R_c, and range between 0.1 and 0.5. At the inlet, the term $(1 + \xi_1)\frac{\rho V^2}{2}$ represents a velocity head loss due to fluid acceleration plus an entrance loss represented by ξ_i. The following numbers for $(1 + \xi_1)$ were obtained from the data of Figure 3.

Stepped Seal Data

R_a	$(1 + \xi_1)$	$(1 + \xi_2)$	$(1 + \xi_3)$
382,000	1.129	.435	.484
323,000	1.129	.432	.531
150,000	1.255	.432	.371
75,000	1.681	.537	-.178
50,000	1.913	.916	.999

These results are fairly regular and constant over the higher Reynolds number sets, but tend to be erratic over the two lower Reynolds number sets. The results for R_a = 75,000 and 50,000 should be viewed with some skepticism because of the previously mentioned accuracy of the pressure transducers. The most unexpected result from Figure 3 is the relatively small pressure gradient across step 1, the entry step, as compared to the remaining two steps. Figures 3(a) and 3(b) show a small pressure rise immediately before the first step, while figure 3(c) shows a flat pressure gradient across the first step. A zero pressure gradient, $\sigma = 0$, would yield a prediction of zero stiffness contribution from the first step.

For a tapered seal, the steady-state leakage relationship is [11]

$$\Delta P = \frac{\rho V^2}{2} \left[\frac{1+\xi}{(1+q)^2} + 2\sigma + 4q\right]$$

for small q. The experimental results from figures 4(a) - (c) yield the following entrance-loss result:

R_a	$1 + \xi$
434,000	0.926
325,000	0.996
150,000	0.878

While these losses are constant, independent of R_c, this is not the case in figures 4(d) and 4(e) where the losses increase steadily with R_c. In fact, an inlet pressure increase was measured for R_c = 16,890 and R_c = 49,981. The tapered-seal results above for high Reynolds numbers are consistent with Fleming's assumption [10] of zero ξ.

Dynamic Results

Only a very limited number of dynamic data sets have been reduced. The only immediate conclusion which has been drawn from these results is that the force magnitude $|R| = (R_\theta^2 + R_r^2)^{1/2}$ is comparable for both the current stepped seal configuration and the proposed tapered seal. A comparison of their radial and tangential forces and a comparison to theory will be forthcoming shortly.

CLOSING STATEMENTS

A test facility has been developed which has the capability for testing annular seals at Reynolds numbers which are comparable to those developed in cryogenic turbopumps. Generally speaking, the facility works the way it was expected to and is beginning to yield the types of static and dynamic test data that are required to support theoretical predictions of seal rotordynamic coefficients and leakage.

REFERENCES

1. D.W.Childs, "The Space Shuttle Main Engine High Pressure Fuel Turbopump Rotordynamic Instability Problem," ASME Trans.J of Engineering for Power,pp. 48-57, Jan. 1978

2. H.F.Black, "Effects of Hydraulic Forces in Annular Pressure Seals on the Vibrations of Centrifugal Pump Rotors," J.M.Eng. Sci., Vol.11, no.2,pp.206-213,1969

3. H.F.Black and D.N.Jensen, "Dynamic Hybrid Properties of Annular Pressure Seals, " Proc. J.MECH. Engin., Vol. 184,pp.92-100,1970

4. H.F. Black and D.N.Jensen,"Effects of High Pressure Ring Seals on Pump Rotor Vibrations,"ASME Paper No. 71-WA/ff-38, 1971.

5. H.F.Black, P.Allaire, and L. Barrett, "The Effect of Inlet Flow Swirl on the Dynamic Coefficient of High-Pressure Annular Seals," Ninth International Conference in Fluid Sealing, BHRA Fluid Engineer Engineering, Leeuwenhurst, The Netherlands, April, 1981.

6. Y.Yamada, "Resistance of Flow through Annulus with an Inner Rotating Cylinder,"Bul.J.S.M.E., Vol.5, no.18,pp.302-310,1962.

7. D.W.Childs, "Dynamic Analysis of Turbulent Annular Seals Based on Hirs' Lubrication Equations," accepted for publication, ASME Trans.J. of Lubrication Technology.

8. D.W.Childs,"Finite-Length Solutions for Rotordynamic Coefficients of Turbulent Annular Seals," accepted for publication, ASME Trans.J. of Lubrication Technology.

9. G.G.Hirs, "A bulk-Flow Theory for Turbulence in Lubricant Films," ASME J. Lubrication Technology, pp. 137-146, April 1973.

10. D.P.Fleming, "High Stiffness Seals for Roter Critical Speed Control," ASME Paper 77-DET-10,Design Engineering Technical Conference, Chicago,IL., 26-30 September 1977.

11. D.W.Childs,"Convergent-Tapered Annular Seals: Analysis for Rotor-dynamic Coefficients," Fluid Structure Interactions in Turbomachinery presented at the ASME winter annual meeting, 15-20 November 1981.

12. R.C.Hendricks,"Some Flow Characteristics of Conventional and Tapered high-Pressure-Drop Simulated Seals," ASLE preprint No.79-LC-3B-2, presented at the ASLE/ASME Lubrication Conference, Dayton, Ohio; 16-18 October 1979

13. D.W. Childs, J.B.Dressman, and S.B.Childs, "Testing of Turbulent Seals for Rotordynamic Coefficients," NASA Conference Publication 2133,Rotordynamic Instability Problems of High Performances Turbomachinery, proceedings of a workshop held at Texas A&M Univ., 12-14 May 1980, pp. 121-138, proceedings published September 1980,

14. W.L. Bowen, and R. Bhateje, "The Hollow Roller Bearing,"ASME Paper No. 79-Lub -15, ASME-ASLE Lubrication Conference; Dayton,Ohio; 16-18 October 1979.

15. H. Stephen and K.Lucas, Viscosity of Dense Fluids, p.59,Plenum Press, New York-London

16. Anon., T-1301,Thermodynamic Properties, Dupont Fire Extinguisher Properties, E.I. Dupont DeNemours & Co., Wilmington, Del; 1966.

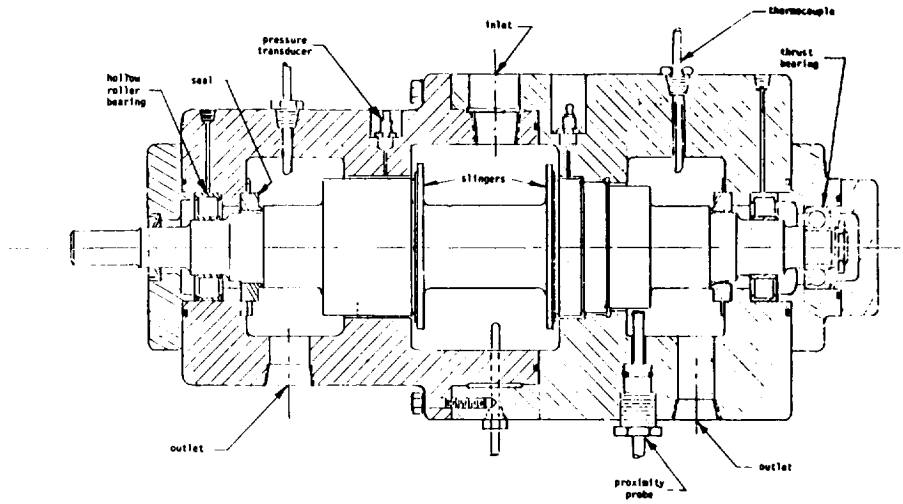

Figure 1. - Test-rig assembly.

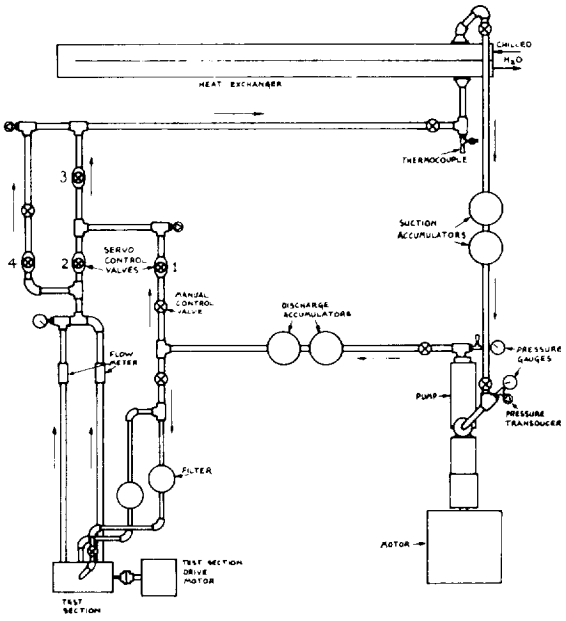

Figure 2. - Test-facility layout.

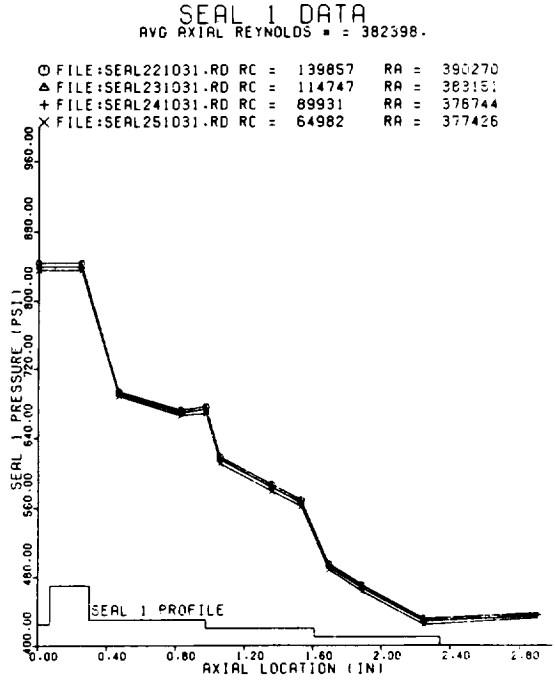

Figure 3(a).

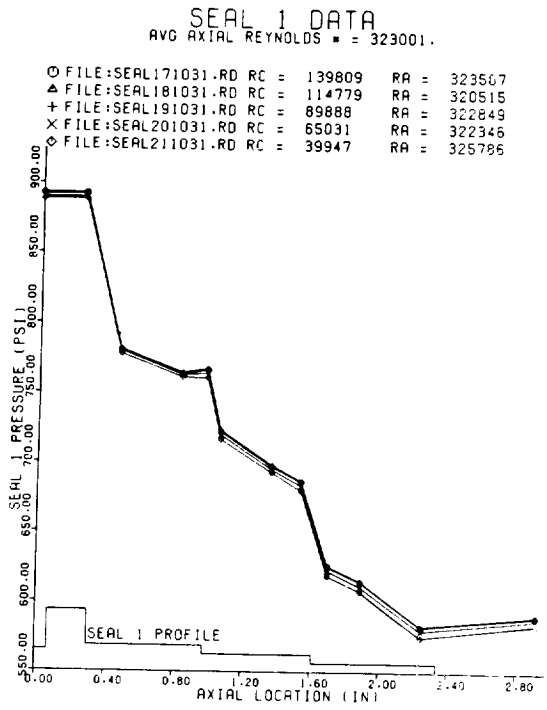

Figure 3(b).

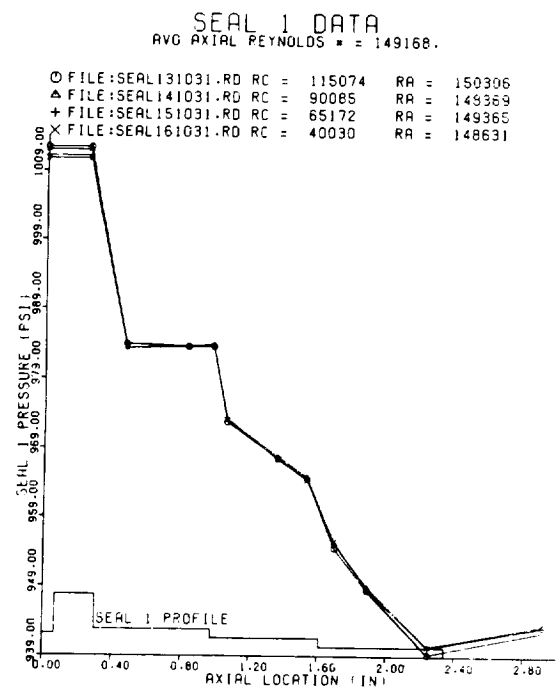

Figure 3(c).

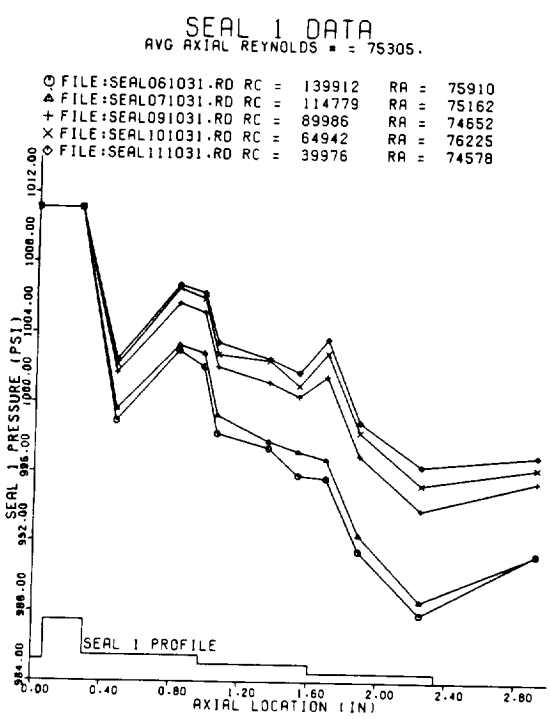

Figure 3(d).

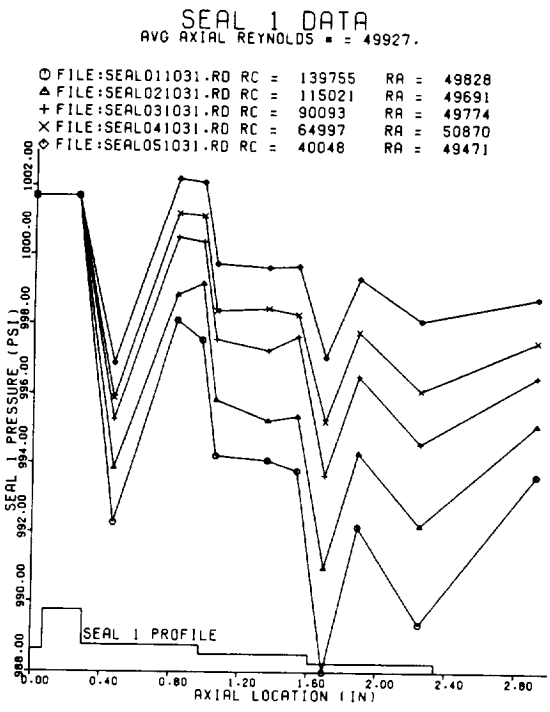

Figure 3(e).

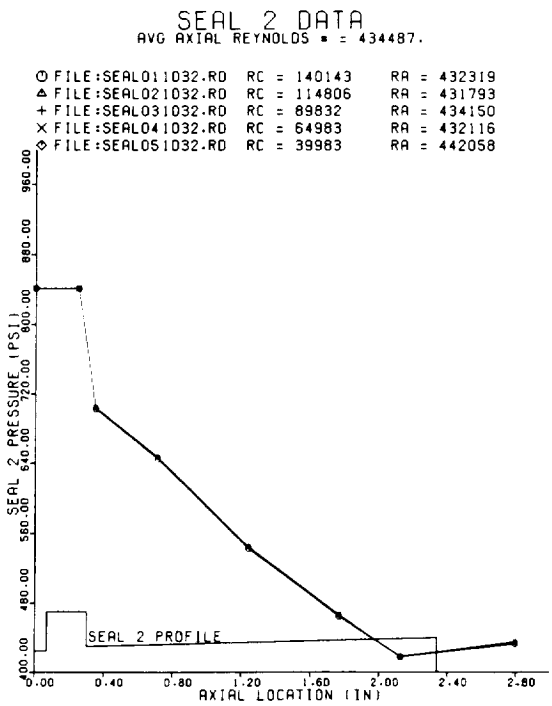

Figure 4(a).

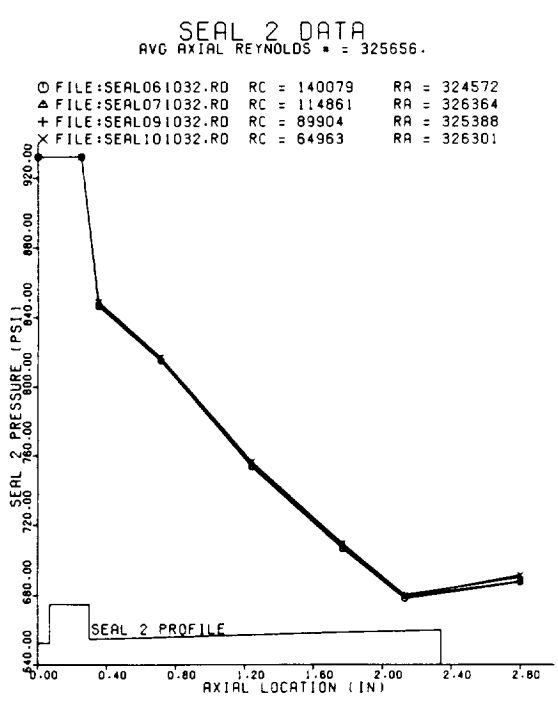

Figure 4(b).

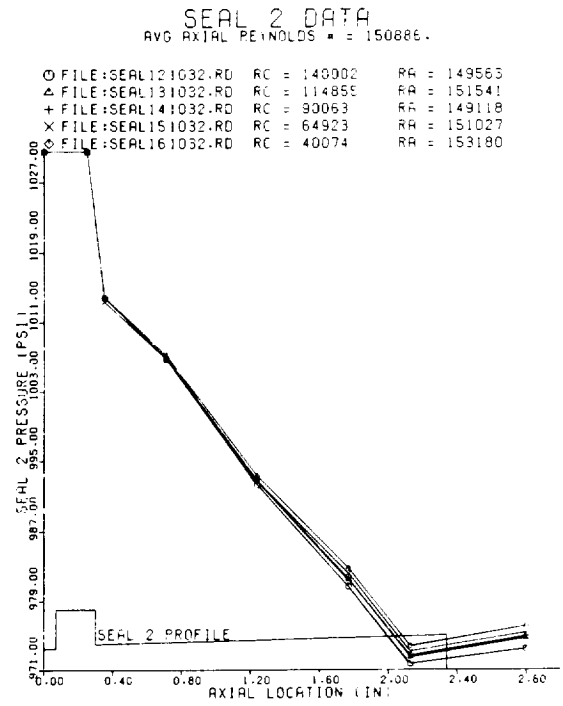

Figure 4(c).

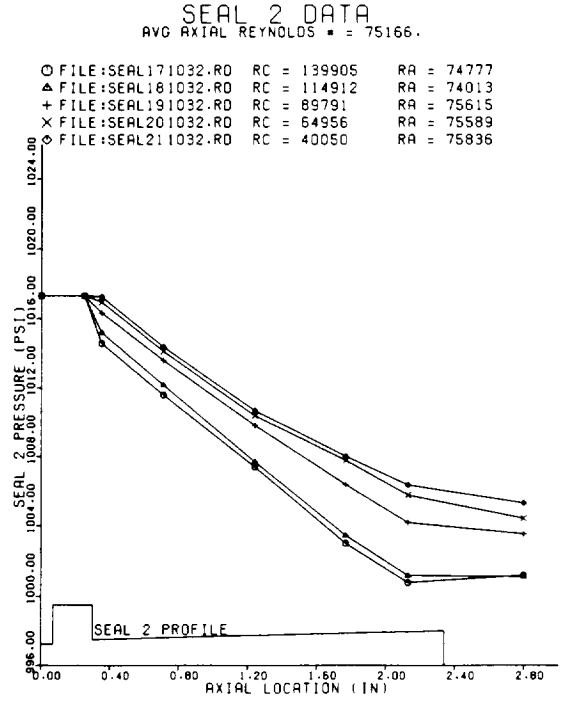

Figure 4(d).

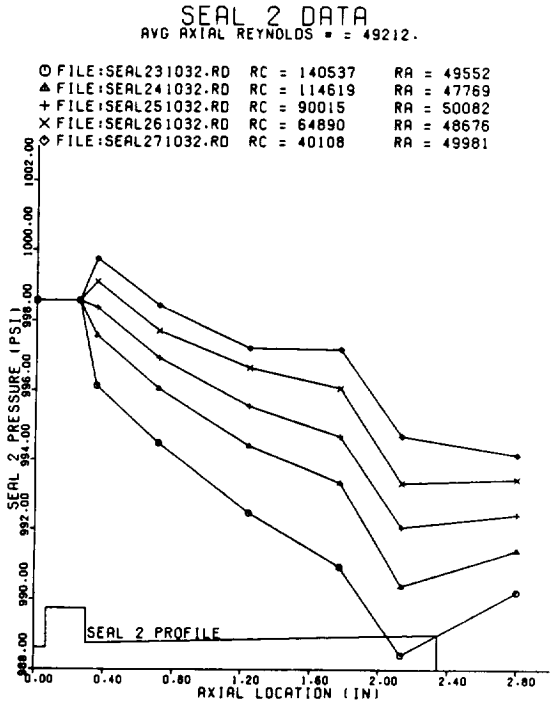
SEAL 2 DATA
AVG AXIAL REYNOLDS # = 49212.
FILE:SEAL231032.RD RC = 140537 RA = 49552
FILE:SEAL241032.RD RC = 114619 RA = 47769
FILE:SEAL251032.RD RC = 90015 RA = 50082
FILE:SEAL261032.RD RC = 64890 RA = 48676
FILE:SEAL271032.RD RC = 40108 RA = 49981
SEAL 2 PRESSURE (PSI)
1002.00
1000.00
998.00
996.00
994.00
992.00
990.00
988.00
SEAL 2 PROFILE
0.00
0.40
0.80
1.20
1.60
2.00
2.40
2.80
AXIAL LOCATION (IN)

Figure 4(e).